Proceedings World Geothermal Congress 2015
Melbourne, Australia, 19-25 April 2015

Natural Permeability in Fractured Triassic Sediments of the Upper Rhine Graben from Deep Geothermal Boreholes

Jeanne Vidal[1], Albert Genter[2], Philippe Duringer[1], Jean Schmittbuhl[1]

Mailing address, [1]EOST, Université de Strasbourg, 5 rue René Descartes, F-67084 Strasbourg Cedex, France; [2]GEIE, Exploitation Minière de la Chaleur, Route de Soultz - BP 40038, F-67250 Kutzenhausen, France

E-mail address, jeanne.vidal@etu.unistra.fr, genter@soultz.net, duringer@unistra.fr, jean.schmittbuhl@unistra.fr

Keywords: Triassic sediments; well logging; fracture zones; permeability; convection; EGS; Upper Rhine Graben

ABSTRACT

The thermal regime of the Upper Rhine Graben (URG) is characterized by a series of anomalies near Soultz-sous-Forêts (France), Rittershoffen (France) and Landau (Germany) where temperatures reach 200 °C at 5 km deep for the deepest investigated drilling site. They are associated with a regional redistribution of heat driven by groundwater circulation in the basement and in the sediments above it. The geothermal fluid is trapped within fractures and faults cross-cutting the Cenozoic and Mesozoic sedimentary cover and taking root in the Paleozoic fractured basement. The present study helps to understand the convective cell structure in order to assess to optimize geothermal borehole trajectory. The analysis of mud logging and geophysical well logging data coming from the Soultz geothermal wells (GPK-2, GPK-3, GPK-4) shows the occurrences of nine fracture zones deeper than 900 m, in the limestones from Muschelkalk (Middle Trias) and the sandstones from Buntsandstein (Lower Trias). Based on indication from partial to total mud losses, those fracture zones have been classified as permeable or not. Permeable fractures lying between circa 900 m deep and 1400 m deep are supposed to be connected to a large scale fault network that controls the top of convective cells. There is no obvious permeability indication in the sedimentary formations above the Keuper layer (Top Trias) as well as the uppermost part of the sedimentary cover which acts as a cap rock insulating the convective regime governing in the Triassic sediments and the granitic basement.

1. INTRODUCTION

The thermal regime of the Upper Rhine Graben (URG) is characterized by a series of geothermal anomalies near Soultz-sous-Forêts (Alsace, France), Rittershoffen (Alsace, France) and Landau (Rhine-Palatinate, Germany). These areas reveal local thermal gradients up to 100 °C/km in the uppermost part of the sedimentary cover attributed to hydrothermal convective cells circulating inside a nearly vertical fracture network in the granite basement and in the Triassic fractured sediments above it (Schellschmidt, 1996 ; Pribnow and Schellschmidt, 2000 ; Pribnow and Clauser, 2000). Interpretation of seismic reflection profiles identifies major large-scale faults cross-cutting the Cenozoic and Mesozoic sedimentary cover and taking root in the Paleozoic fractured basement (Cautru, 1988) (Figure 1). Hydrothermal pathways in the sub-vertical faults network within the granitic basement are confirmed by thermo-hydraulic model (Le Carlier et al., 1994 ; Kohl et al., 2000; Baechler et al., 2003). On the thermal profile in deep Permo-Triassic sediments and in the crystalline basement, the convective regime (5 °C/km) is illustrated by the occurrence of negative thermal anomalies corresponding to natural fractured zones (Genter et al., 2010). Those cooled zones due to mud or water invasion by drilling or stimulation operations may be interpreted as a thermal expression of permeable faults. However they are not noticeable in the sedimentary cover between 0 and 1 km deep where the dominating thermal regime remains highly conductive. The present paper focuses on the transitional zone located between 0.8 and 1.2 km deep (Figure 2). This depth section is at the intersection between the uppermost conductive part (0-1.0 km) and the underlying convective zone (1.0-3.5 km).

The sediment/basement interface is therefore very challenging for industrial exploitation, the heat being carried in the geothermal fluid circulating within natural fractures. Several Enhanced Geothermal System (EGS) projects in the URG target geothermal reservoirs in this depth zone located between the bottom of the sedimentary cover and the top of granitic basement corresponding to the top of the convective cells. For example geothermal wells drilled in the fractured Muschelkalk layer in Southern Germany (Offenbach or Speyer) for EGS projects were targeted to produce brine with acceptable temperatures for electricity production (Kreuter et al., 2003, Stober et al., 2009 ; Stober et al., 2011). Other projects at Cronenbourg, at Rittershoffen (France), at Landau, at Insheim and at Bruchsal (Germany) demonstrate the quality of the resource in the fractured sediment/basement interface for geothermal use (Housse, 1984; Baumgärtner et al., 2013; Hettkamp et al., 2013; Villadangos, 2013).

The aim of this study is to significantly contribute to a better understanding of geological structures of convective cells. We based our geological analysis of the sediment/basement interface on drilling, geological and geophysical data available at the Soultz geothermal wells. Indeed the work was concentrated on a detailed interpretation of geophysical and geological logs from the Soultz geothermal wells GPK-2 (5 km), GPK-3 (5 km) and GPK-4 (5 km) mainly between the topographic surface and the Triassic formations, lying between 0.8 and 1.4 km deep. The available drilling data are the lithology, rate of penetration of drilling bit, weight on bit, evidences of natural outflow (partial and total mud losses), occurrences of gas (helium, methane) and mud temperature variations. Additional well logging data such as temperature logs, gamma ray and caliper logs were correlated with drilling data. Based on those well logging data, the location in the sedimentary cover of the fracture zones and their permeability were used to estimate the impact of the fracture system on the thermal regime. Properties of the fracture system limit hydrothermal circulations and we tried to identify a sedimentary layer which could limit the upper part of the convective cells. Spatial correlation of the fracture zones between different geothermal boreholes is an important issue of this study for exploring the heterogeneity of the permeability of a given fault crossing several wells at depth.

After presenting the Soultz geothermal reservoirs and a description of geological and thermal background, well logging data in Soultz geothermal boreholes will be evaluated in order to highlight fracture zones in the sedimentary cover. Then the temperature profiles will be analyzed in order to assess the thermal expression of fracture zones in the conductive part. Finally a schematic conceptual model of the convective cell structure will be proposed.

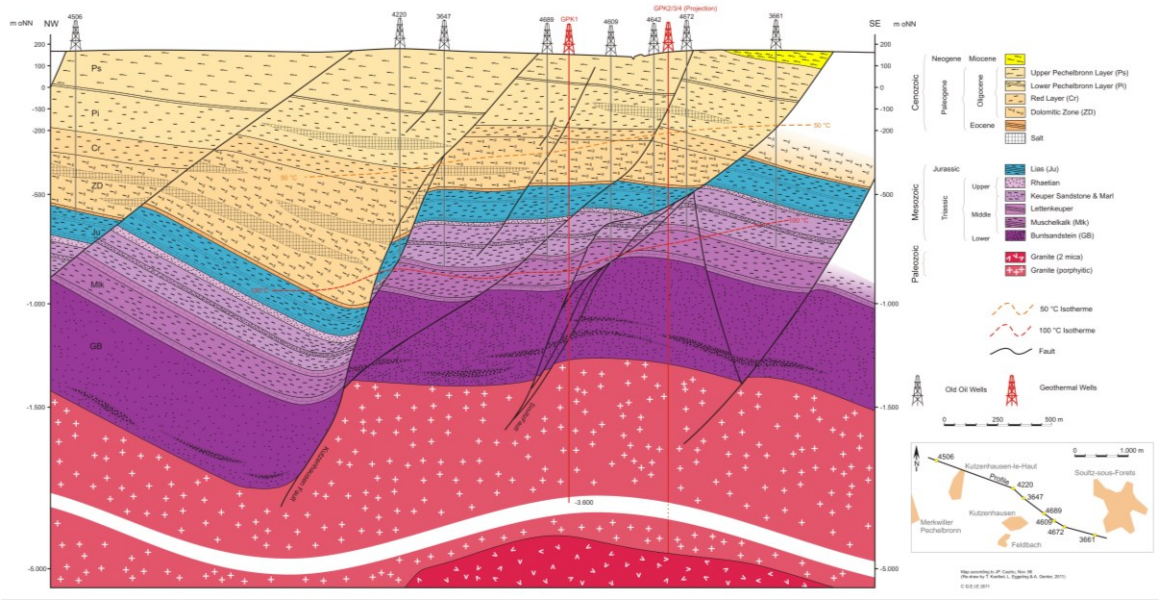

Figure 1: Geological cross section based on seismic reflection profiles (after Cautru, 1988, redraw by Koelbel et al., 2011). Oil wells are projected on the cross section as well as the geothermal boreholes GPK-1 and GPK-2.

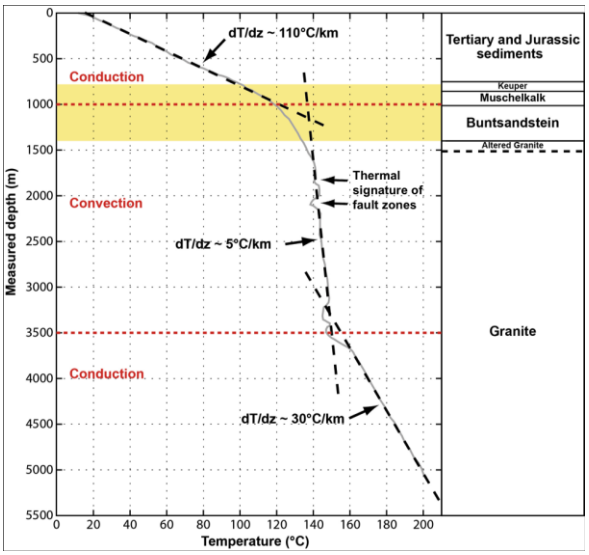

Figure 2: Equilibrium temperature profile obtained from log run in GPK-2 several months after drilling operation finished. Main geological units are presented versus depth. The yellow rectangle symbolized the zone of the top of the convection, the target of the study.

2. PRESENTATION OF THE EGS SITE OF SOULTZ-SOUS-FORÊTS

2.1 The So-called "Soultz Geothermal Anomaly"

At regional scale, the temperature distribution is spatially not homogeneous and series of local anomalies with temperatures above 140 °C at 2 km deep are mainly concentrated on the western side of the URG as Soultz-sous-Forêts (France), Landau (Germany) or Mainz (Germany) (Baillieux et al., 2013; Schellschmidt, 1996). The temperature anomalies in the URG are controlled by three thermal relevant mechanisms: variability of radiogenic heat production, convection and conduction. The so-called "Soultz geothermal anomaly" is one of the most important temperature anomalies and was the subject of numerous studies. Soultz granites offer an optimal radiogenic production of 5.5-6.5 $\mu W/m^3$ measured on core samples from GPK-1 well (Rummel et al., 1988) and an important vertical variation of 2-7 $\mu W/m^3$ in GPK-2 well (Pribnow and Schellschmidt, 2000). However this radiogenic production is insufficient to explain the geothermal anomalies (Stussi et al., 2002). A detailed observation of geothermal anomaly at kilometric scale reveals a concentration of hot zones along Soultz or Kutzenhausen normal faults and is attributed to hydrothermal circulation

per ascensum, within the crystalline basement and the sandstones, based on temperature data from various oil and geothermal wells (Benderitter et Elsass, 1995; Pribnow and Clauser, 2000; Pribnow and Schellschmidt, 2000). To explain Soultz anomaly, various hydro-thermic modeling have been done at Soultz horst region (Kohl et al., 2000) as well as on several cross sections perpendicular to the graben axis (Le Carlier et al., 1994; Person and Garven, 1992; Guillou-Frottier et al., 2013).

The typical thermal profile run in the 5-km deep wells at thermal equilibrium conditions, shows a temperature of 200 °C at 5 km deep (Figure 2). This profile could be divided into three parts. The uppermost part from 0 to 1 km in sedimentary formations from Tertiary and Secondary (Jurassic and Upper Trias) shows a linear geothermal gradient of 110 °C/km that indicates a conductive heat transport mechanism (Pribnow and Schellschmidt, 2000). This geological section acts like a cap rock, i.e. an impermeable layer which insulates the hydrothermal system active below. The part from 1 to 3.5 km deep composed by deep sedimentary formations (Buntsandstein and Permian sandstones) and by granitic basement exhibits a very low geothermal gradient of 5 °C/km which characterizes a convection mechanism. This second thermal unit is locally disturbed by cold fractured zones, for example at 1.6 km deep or 2.1 km deep, which can be interpreted as remnant cooling from drilling or from massive hydraulic injections (Genter et al., 2010). Permeable fractured and altered zones are cooled by invasion of drilling mud invasion or of fresh water during hydraulic stimulation operations. Fractures in the granitic basement have a negative thermal signature visible even several months after hydraulic operations. Finally the innermost part only composed by crystalline formations beyond 3.5 km deep where the gradient is linear again and about 30 °C/km that indicates a control of a conductive regime.

2.2 Soultz Reservoirs

The target of the Soultz project was the development, the hydraulic testing and the modelling of two EGS reservoirs within the granitic basement at 3.5 and 5 km deep (Gérard et al., 2006; Dezayes et al., 2005). The different phases of the Soultz project have provided a rich and diverse database of the granitic basement. However the knowledge of the 1.4 km overlying Cenozoic and Mesozoic sediments is much poorer. In spite of intensive investigations in the uppermost part during the oil production of the Merkwiller-Pechelbronn oil field, the geothermal exploration was focused on the granitic basement. Three geothermal boreholes were drilled into the crystalline basement; GPK-2, GPK-3 and GPK-4 (Figure 3). Geothermal water is pumped from the production well (GPK-2) and re-injected at lower temperature into the injection wells (GPK-3 and GPK-4) after delivering its geothermal energy through a heat exchanger to a binary power plant (Genter et al., 2013). At Soultz, two other wells penetrated the granite massif and thus its sedimentary cover: an exploration geothermal borehole GPK-1, an older petroleum well deepened at 2.2 km deep, called borehole EPS-1 (2.2 km deep). In both of them, core samples in Triassic sediments have been collected (Degouy et al., 1992).

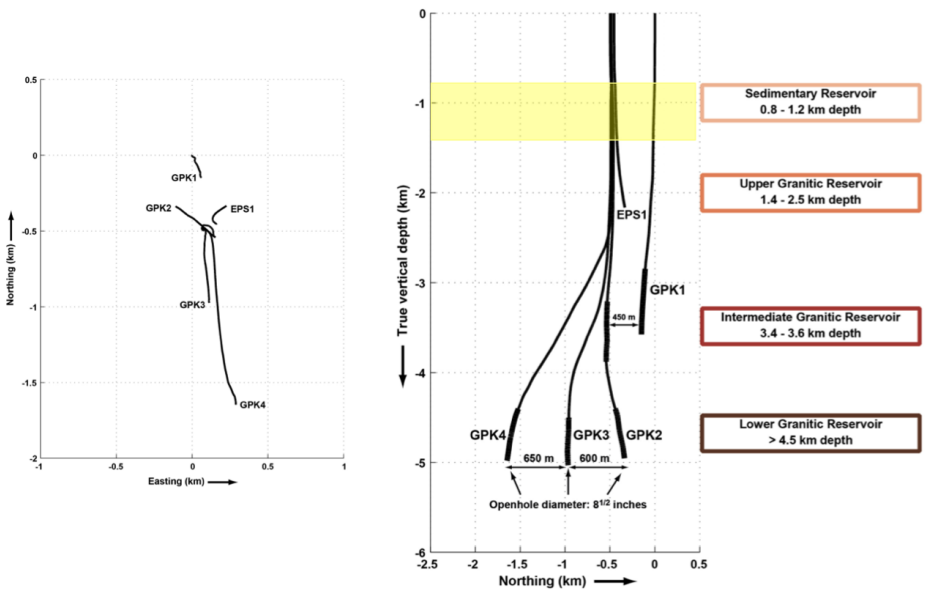

Figure 3: Local map view of the Soultz site and South-North vertical cross section showing the trajectories of the deep geothermal wells GPK-2, GPK-3 and GPK-4 and also the exploration wells GPK-1 and EPS-1. The location of the different sedimentary and granitic reservoirs are also indicated.

Below the sediments, the crystalline basement is encountered from 1.4 km to 5.0 km deep (Figure 1) and presents several indications of convection associated to the fracture system at different scales, from micro-cracks to local faults. From core analysis and well logs interpretation, natural fractures within the granite were shown to be clustered in hydrothermally altered and fractured zones (Genter et al., 2000). Moreover, the natural fracture system directly controls producing zones of geothermal fluid or drilling mud loss zones (Vuataz et al., 1990; Evans et al., 2005). Strong hydrothermal alteration is an evidence of paleo-circulations which have resulted in dissolution of the primary minerals such as biotite and plagioclase (Genter et al., 1989, Genter et al., 2000). However fracture zones present both permeability and sealing related to deposition of altered minerals such as secondary quartz, clay minerals, calcite or sulfides (Genter and Traineau, 1992; Genter and Traineau, 1996; Genter et al., 1997) (Figure 4). Traces of organic matter in a fracture zone EPS-1 reveal the hydraulic communication between basement and sediments (Ledésert et al., 1996).

A detailed analysis of image logs, standard geophysical logs, petrographic logs and flow logs shows a clear spatial relationship between the occurrence of natural permeability and hydrothermally altered and fractured zones in granite (Evans et al., 2005 ; Dezayes et al., 2010). Natural brine circulates within subvertical fracture system between the deepest crystalline reservoirs and the shallowest sedimentary reservoir. This paper focuses on a detailed analysis of various borehole data (mud logging, geophysical logs) in the Triassic reservoir between 0.8 and 1.2 km deep.

Figure 4: Core sample in sandstones from Buntsandstein at 1204 m deep in the well EPS-1 showing a fracture zone with several individual fractures filled by barite and galena. The diameter of the core sample is 7.6 cm.

2.3 Geology of the Sedimentary Cover

In GPK-2 well, the Tertiary section, from the topographic surface to 623 m deep, is composed at the uppermost part by claystones and marlstones from Pechelbronn oil formations aged of Oligocene (316 m deep) (Cautru, 1988; Ménillet, 1976) (Figure 1). The Eocene formations are divided into two types of marlstones; the ferruginous marlstones from Red Layer (353 m deep) and marlstones interbedded with dolomite layers from Dolomitic Zone (601 m deep), and end with a thin layer of dark claystones. This Tertiary section presents an erosional contact with the Jurassic formations. Dark-grey claystones with the presence of calcareous shale composed the Dogger formation (653 m deep) and then Lias formation is marked by grey silty calcareous claystones (763 m deep). The innermost part of the sedimentary cover is a classical Germanic Trias with dolomites, anhydrite and clays for Upper Triassic layers; the Keuper formation down to 853 m deep and the Lettenkohle formation down to 873 m deep. Then Muschelkalk formations are located down to 1021 m deep. The detailed stratigraphy of Muschelkalk and Buntsandstein can be specified thanks to core sample analysis from EPS-1. Stratigraphic series from the classical Germanic Trias show a rather constant thickness through all the URG and all formations can be easily correlated between boreholes even if separated by several kilometers. The Upper Muschelkalk starts by massive limestones rich in Terebratula. Then marly calcareous formations spread over 35 m before massive crinoidal limestones beds. Those limestones are defined as the most competent rocks of the sedimentary cover with a high carbonate content. They are about 14 m thick and mark the transition to the Middle Muschelkalk. The central section of Muschelkalk is marly dolomites characterized by the invasion of anhydrite (circa 50 m thick). The Upper Muschelkalk begins circa 980 m deep and is divided into two parts; the uppermost part is marly calcareous dolomites and the innermost part is sandstones rich in fossils. The sedimentary cover ends with the sandstones from Buntsandstein down to 1405 m deep. At the top of the formations, the Voltzia sandstones defined as clayed and fine-grained spread over 10 m. The sandstones below are distinguished by bigger grain size and belong to the section called Intermediate Layers (about 40 m thick). Vosgian sandstones are typical medium-grained to conglomeratic continental sandstones with clay formations and composed the Middle Buntsandstein. The last 50 m of the formation are composed by Annweiler sandstones, an argilaceous red sandstone. This transitional layer of Permian sandstones is visible on core samples of EPS-1 well but hardly noticeable from cuttings. Porosity evaluated in Buntsandstein is quite low with 10 % at the top of the formation and 20 % for the Vosgian sandstones (Vernoux et al., 1995). Petrophysical studies on core samples point out the role of the matrix permeability which control geothermal fluid circulations through these sandstones (Haffen et al., 2013).

3. METHODOLOGY OF THE STUDY

3.1 Fracture Zone Location in Wells

We conducted a comprehensive borehole data analysis from the Soultz geothermal boreholes. We used drilling mud logging data such as drilling mud losses, natural outflow, gas content, Rate of Penetration (ROP) collected during drilling operations. Geophysical well loggings such as caliper and Gamma Ray (GR) have been also used and compared to mud logging data. The depth match interval of about - 4 m between the drilling mud logging data and the geophysical well logging data must be taken into account. In order to avoid to depth match artificially upward or downward those datasets, it was decided to keep data in their own depth referential. Even if sedimentary cover was not the main target of the geothermal exploration at Soultz, mud logging data and well logging data such as calipers and GR have been collected properly in the geothermal wells GPK-2, GPK-3 and GPK-4 (Baumgärtner et al., 1995; Baumgärtner et al., 2000; Baumgärtner et al., 2005; Hettkamp et al., 2004). For those three geothermal wells, temperature logs have been run behind the casing at equilibrium thermal conditions. In each geothermal well, available borehole data were spatially correlated with depth in order to highlight some physical variations interpreted as fracture zone. Three kinds of fracture zone have been outlined:

- Permeable fracture zone is defined with the occurrence of drilling mud losses or natural outflow or helium gas content. The best permeability indicator during drilling operations is mud total losses. Generally in such conditions, calipers and ROP increase simultaneously at the same depth location.
- Sealed fracture zone is defined by absence of clear indication of mud losses or natural outflow. However fracture zone is defined by caliper enlargement or ROP increase.
- Partially sealed fracture zone is an intermediate group between permeable and sealed fracture zone. Indeed in some cases, there is a clear indication of fracture zone occurrence (caliper or ROP increase), but permeable indicators are poorly constrained. For example mud logging data are mainly qualitative and thus it introduces a certain amount of uncertainty on the permeability range.

As the wellhead of GPK-2, GPK-3 and GPK-4 are very close (less than 15 m) and as they are sub-vertical in the similar sedimentary section, we conducted some spatial correlation of fracture zones. In order to compare fracture zones in wells, a similar terminology and labeling for fracture zones has been used for the three geothermal wells.

3.2 Typology of Data

The first group of well log data is instantaneous well logs like the ROP that is the speed at which the drilling bit enters in the rock, usually reported in m/hr. Normally drill bit data show a speed decreasing as the drill bit bores into denser formations. At Soultz the mean speed is 8 m/hr in soft sediments (above 1 km deep) and 5 m/hr in hard sediments (below 1 km deep) and 2 m/hr in the granite. When the ROP is higher than the mean value, it is generally interpreted as the effect of a localized fracture zone. In such case, the driller is obliged to reduce the Weight On the Bit (WOB) in order to drill in stable drilling conditions. The WOB is the mass of the tool strings that applies a vertical load on the drilling bit and ranges, in the Soultz case, from 11 tons in soft sediments to 15 tons in hard Triassic sediments or granite. If WOB is reduced by driller, the ROP is artificially low but could characterize a fracture zone. Flow variations represent the amount of mud circulation and can be interpreted as a loss (outflow). Mud, also called drilling fluid, refers to fluids that contain significant proportion of suspended solids in water solution. When the drilling bit crosses a permeable fracture zone, the well records a partial decrease of the outflow or a even total losse of mud circulation. Variations of mud temperature, recorded in Celsius degrees, suggest mixing between hot geothermal fluid and cold drilling mud. Like for the natural outflow, the permeable fractures bearing hot fluid could induce drastic variation of the drilling mud temperature.

Mud logging also includes the monitoring of natural gas emission. It is a classical method for fracture zones detection already shown at Soultz where helium gas anomalies are associated with permeable fractures at 1810 m deep in the granite part of GPK-1 well (Vuataz et al., 1990). Alkcan gas content such as methane could be interpreted as fluid circulation in local fracture zones or as an indicator of matrix permeability. For reference, helium, methane and ethane content in the atmosphere is about 5.24 ppm, 1.75 ppm and 0.50 ppm respectively.

The second group of well logging data is wireline logs measured continuously while the tool is moving upward from the bottom of the borehole and transmitted through a wireline to surface. For this study, standard geophysical wireline logs were used as the GR measuring the natural radioactivity of the geological formations in the borehole and reported in gAPI. At Soultz, the spectral gamma ray measurement was a significant proof of hydrothermally altered and fractured zone occurrences in granite (Hooijkaas et al., 2006). It is more difficult to use this method to localize fracture zones in Triassic sediments due to their lower content in radioisotopes. In the Lettenkohle and in the Upper Muschelkalk, the local minima of GR are associated to the marly calcareous formations. In the Buntsandstein, clay layers (lower than 2 m thick) correspond to isolated and localized GR peaks. Peaks associated to fracture zones with hydrothermal alteration halo in granite show a larger variation of GR than those induced by sedimentary clay layers. In a fracture zone, the caliper which measures the borehole diameter, is not circular anymore and presents a cave phenomenon. With standard geophysical logs such as 6-arm caliper, several individual peaks visible on each curves are very helpful for characterizing a given fracture zone (Figure 5, Zone1). In some case, ROP increase fits in depth with caliper enlargement re-enforcing the occurrence of fracture zone.

4. CHARACTERIZATION OF FRACTURE ZONES IN THE WELLS

4.1 Well GPK-2

The synthetic log of GPK-2 shown in Figure 5 contains lithology, stratigraphy, GR and calipers. The caliper was a 6-arm tool measuring 6 radii or 3 diameters that correspond to C14, C25 and C36 curves. The nominal diameter of the well is $12^{1/4}$ inches when the wellbore is not affected by caving or ovalization. ROP is lacking locally because digital data were only available in the granite section. It presents also permeability indicators, mud losses and helium or methane gas enrichment.

The depth section of the synthetic log was focused at the sedimentary part where permeability indicators were detected, i.e. between 890 and 1280 m deep (Figure 5). In this depth section, eight fracture zones have been highlighted from well logging data. The zones Z1, Z2 and Z9 are deduced from mud losses information and helium anomaly correlated spatially with the local caliper enlargement. The zones Z3, Z5, Z6, Z7 and Z8 are hypothesized from local caliper or ROP variations. Thus they are interpreted in terms of sealed fractures or fracture zones with no permeability indication during drilling.

Zone Z1 presents total mud losses and is permeable. Several individual peaks are visible on calipers from 907 and 913 m deep with a maximum of 16.60 inches for C36 at 908 m deep. Considering the nominal diameter of 121/4 inches at this depth, the well diameter is widened of 4.45 inches at the zone Z1. Helium measurements reach 73 ppm at 911 m deep, which is 14 times higher than the helium atmospheric value. Zone Z1 shows clearly the depth match of circa - 4 m between the drilling mud logging data and the geophysical well logging data (Figure 5). The helium peak visible at 911 m deep fits with the caliper anomaly visible at 908 m deep. Surprisingly, ROP is stable. Zone Z1 is a complex permeable fracture zone.

Zone Z2 is a complex structure extending vertically from 943 to 965 m deep. Caliper shows a big perturbation zone with a maximum of 16.60 inches at 948 m deep for the diameter C25, an enlargement of 4.45 inches. ROP values are higher than 50 m/hr at 953 m deep and fit spatially with helium occurrences of 25 ppm. Persistent mud losses are recorded from 955 m deep (20 m^3/h)

to 1030 m deep (5 m^3/h). The relatively high value of gamma ray (104.34 gAPI and 223.25 gAPI at 945 m deep and 963 m deep respectively) is interpreted as a brecciated fault zone filled with clays affecting the Middle Muschelkalk. Zone Z2 is a complex fracture zone showing obvious permeability indicators.

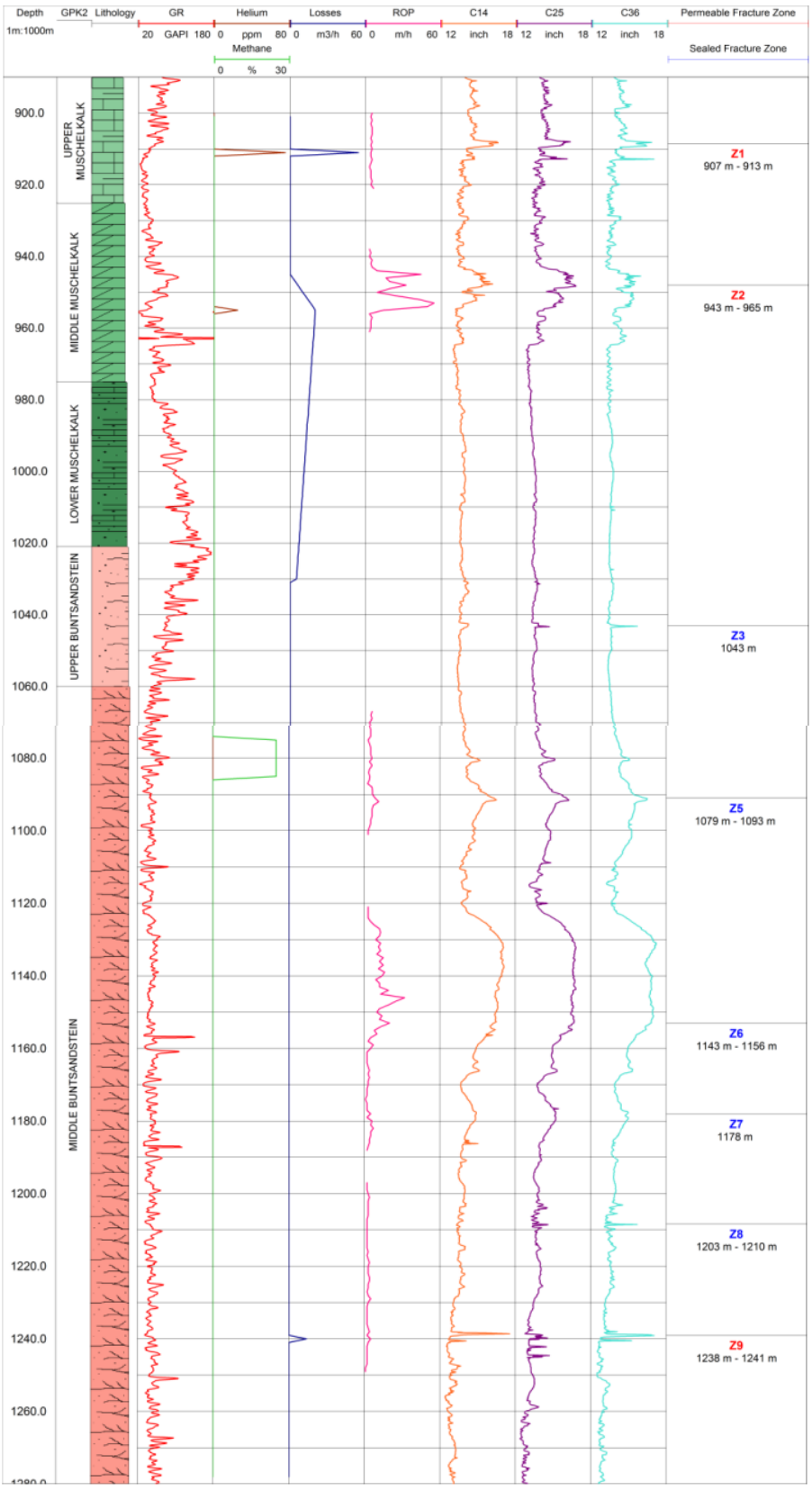

Figure 5: Synthetic log of GPK-2 presenting the lithology, mud losses, GR, gas occurrences (helium and methane), ROP and calipers (C14, C25, C36). Fracture zones are indicated Z1, Z2, Z3, Z5, Z6, Z7, Z8 and Z9. Permeable zones are in red and sealed ones are in blue. Depths are expressed in Measured Depth.

Caliper variations at zone Z3 are very local presenting a sharp peak on three calipers with a maximum of 15.56 inches on C36 at 1043 m deep. This fracture zone is a single non permeable fracture.

Zone Z4 is not visible on GPK-2.

Zone Z5 is characterized by noticeable positive anomalies on the 3 caliper curves from 1079 to 1093 m deep. The maximum caliper variation of 16.18 inches on C25 at 1091 m deep fits with a ROP positive anomaly of 11.50 m/h at 1092 m deep. The peak of methane extends vertically between 1075 to 1089 m deep. As the methane variation is larger than discrete peaks of caliper, it could related only to an organic compound present in the matrix sandstones. Zone Z5 corresponds to a sealed complex fracture zone.

Caliper variations at zone Z6 extends from 1143 to 1156 m deep. It is the highest enlargement of the well GPK-2 in the sedimentary part (5.25 inches at 1130 m deep) and it could be related to the lithological nature of the formations. The ROP positive anomaly presents a maximum of 32.40 m/hr at 1146 m deep. As there is no evidence of mud losses or helium anomaly, the zone Z7 is a sealed fracture zone.

Zone Z7 shows a caliper variation on the three curves. On C25, the maximum of 15.46 inches is observed at 1176 m. There is no anomaly on mud logging data, thus zone Z7 is an individual sealed fracture.

Zone Z8 is visible on calipers with a series of positive anomalies between 1203 and 1210 m deep and a maximum of 14.54 inches on C36 at 1203 m deep. As for Z7 there is no evidence of permeability indicators and thus Z8 has been interpreted as a complex sealed fracture zone.

The latest zone Z9 is characterized by mud losses of 14 m^3/hr recorded at 1240 m deep. The caliper values match at the same depth with several peaks and a major anomaly of 16.80 inches at 1238 m deep. Zone Z9 is a complex permeable fracture zone.

4.2 Well GPK-3

The synthetic log of GPK-3 presented contains lithology, GR, ROP, natural inflow and outflow and temperature inflow and outflow, and calipers, called RD1 to RD6. Between 890 and 1280 m deep, the nominal diameter is $17^{1/2}$ inches. For GPK-3, helium and methane survey were monitored only in the granitic section of the well that means below 2 km deep. Mud losses indicated come from daily drilling report (dark blue curve) and from Hettkamp et al. (2004) (light blue section). In total, eight zones have been highlight: the zones Z1, Z2, Z4 and Z9 thanks to mud losses recorded by the drilling company and zones Z3, Z6, Z7 and Z8 were assumed if at least two well logging parameters present a significant variation.

Zone Z2 is a complex structure with several positive anomalies visible on ROP curve with a maximum of 42.52 m/hr at 950 m deep matching with mud losses with about 32.40 m^3/h at the same depth (Figure 6). The GR value of 98.97 gAPI at 950 m deep is an additional indication of fracture zone with clay deposition. Calipers are also affected with 13.94 inches on RD4 at 951 m deep and 13.18 inches on RD5 at 952 m deep. These values correspond to a diameter of 24.60 inches and thus an enlargement of 7.10 inches. As there is no variation on mud logging data, this zone is a complex permeable fracture zone affecting Middle Muschelkalk formations.

Zone Z9 is characterized by mud losses from 1245 m deep and caliper variation with a maximum of 10.84 inches at 1248 m deep. Surprisingly the ROP is flat (Figure 7). Z9 is permeable fracture zone extending vertically from 1246 and 1250 m deep.

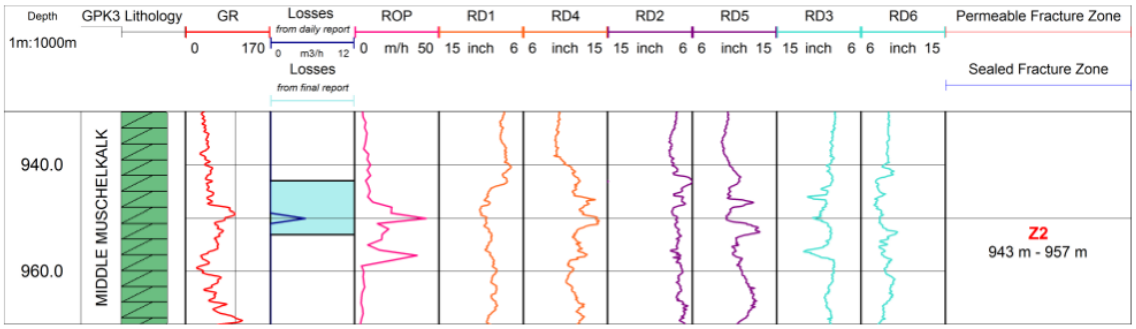

Figure 6: Zoom of the synthetic log GPK-3 between 930 m and 970 m deep presenting the fracture zone Z2 in Muschelkalk formations.

4.3 Well GPK-4

The synthetic log of GPK-4 contains lithology, ROP data, inflow and outflow temperatures, natural outflow and also methane and ethane occurrences monitored by the driller and a service company in the sedimentary part of the well. Calipers and GR data were collected between surface and top basement. The caliper was a 2-orthogonal-arms tool with two measurements CAL1 and CAL2. The nominal diameter between 890 and 1280 m deep was $17^{1/2}$ inches. Occurrences of four zones have been highlighted in GPK-3.

As for GPK-2 and GPK-3, zone Z2 has been correlated thanks to the mud losses. Zone Z2 is a complex structure with several peaks visible between 945 and 957 m deep on ROP (124.86 m/hr at 954 m deep) and caliper data (21.91 inches on CAL2 at 952 m deep) (Figure 8). Zone Z2 is permeable because 4 m3/hr losses were recorded at 956 m deep and persist until 1012 m deep. The clear detachment of 80.30 gAPI of the GR curve from 948 to 955 m deep is also a permeability indication. Z2 is a complex permeable fracture zone.

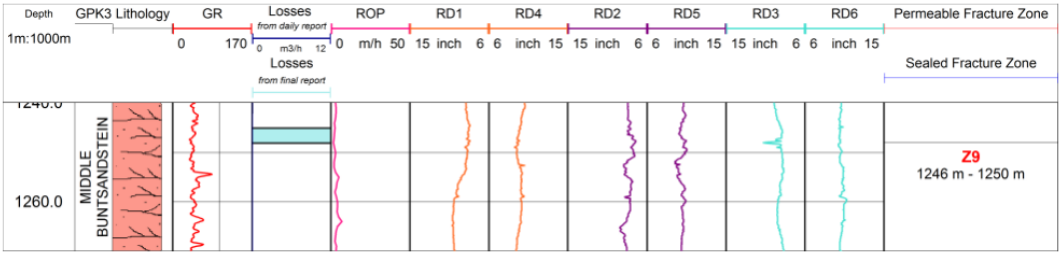

Figure 7: Zoom of the synthetic log GPK-3 between 1240 m and 1270 m deep presenting the fracture zone Z2 in Buntsandstein formations.

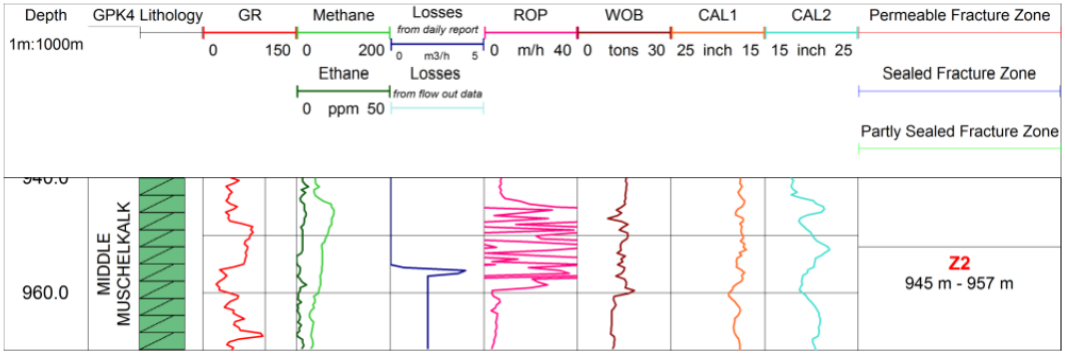

Figure 8: Zoom of the synthetic log of GPK-4 between 940 m and 970 m deep presenting the fracture zone Z2 in Muschelkalk formations.

Zones Z4, Z6 and Z9 were suggested if at least two well logging data present significant variations. For example zone Z9 presents a weak enlargement between 1230 and 1238 m deep with a maximum of 19.47 inches on CAL2 at 1233 m deep (Figure 9). ROP is abnormally flat at the same depth section. Methane curve presents a large detachment of 100 ppm suggesting permeability. Zone Z9 is a partly sealed fracture zone.

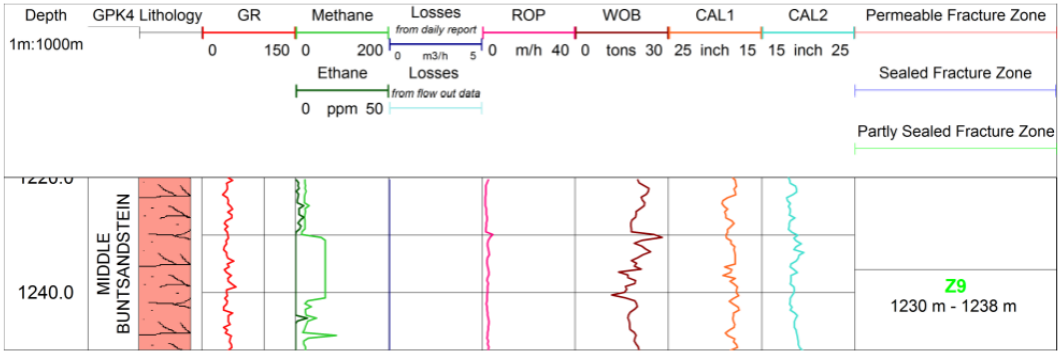

Figure 9: Zoom of the synthetic log of GPK-4 between 1220 m and 1250 m deep presenting the fracture zone Z9 in Buntsandstein formations.

5. CORRELATION OF PERMEABILITY BETWEEN THE WELLS

We did spatial correlation for fracture zones permeability in the geothermal boreholes GPK-2, GPK-3 and GPK-4. In total, nine fracture zones have been identified with permeability indication or not (Table 1). Two zones have been located in the Muschelkalk formations with both indication of permeability (Figure 10). These two zones present a complex structure and show an apparent thickness between 5 and 20 m (Figure 5, Figure 6, Figure 8). They are composed of many individual fractures partly filled by hydrothermal deposition. Zone Z1 cross cuts GPK-2 and GPK-3 whereas zone Z2 cross cut the three wells. As image logs have not been acquired in Muschelkalk, it is rather difficult to derive a 3D organization of those thick structures visible at the same depth in closely spaced vertical boreholes.

Seven fracture zones have been interpreted in the Buntsandstein formations. Four zones do not show clear permeability indication (Z3, Z5, Z6, Z8) whereas Z9 is a complex permeable fracture zone observed on three wells with evidence of natural outflow in GPK-2 and GPK-3. Zone Z4 is permeable only in GPK-3 and zone Z7 is permeable in GPK-3 and GPK-4. Sealed fracture zones correspond to both single fracture (Z3, Z4, Z7) and complex structure (Z5, Z6, Z8). Zone Z6 is the only sealed fracture zone which

crosses the three wells (Figure 10). All other sealed fracture zones in Buntsandstein are visible in two wells except Z5 only visible in GPK-2. In Buntsandstein formations, the complex permeable fracture zone Z9 visible in GPK-2, GPK-3 and GPK-4 could fit with a branch of Soultz fault visible at Soultz scale (Figure 5, Figure 7, Figure 9).

Table 1: Permeability Permeability properties of fracture zones detected in Muschelkalk and Buntsandstein formations in the geothermal boreholes GPK-2, GPK-3 and GPK-4.

Formation	Zone	GPK-2	GPK-3	GPK-4
Muschelkalk	Z1	Permeable	Permeable	
	Z2	Permeable	Permeable	Permeable
	Z3	Sealed	Sealed	
Buntsandstein	Z4		Sealed	Partly Sealed
	Z5	Sealed		
	Z6	Sealed	Sealed	Sealed
	Z7	Sealed		Permeable
	Z8	Sealed	Sealed	Sealed
	Z9	Permeable	Permeable	Partly Sealed

Fracture zones derived from mud logging and geophysical data in the Muschelkalk and Buntsandstein are not observed on the thermal profile done at equilibrium (Figure 2).

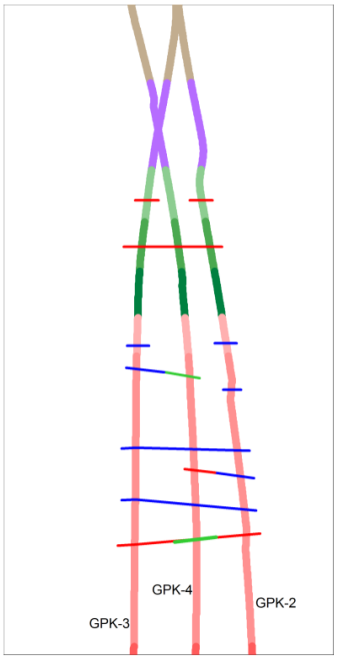

Figure 10: South-North cross-section through the Soultz site showing the fracture zones located on GPK-2, GPK-3 and GPK-4 (named Z1 to Z9) between 800 and 1300 m depth. Permeable zones are in red, partly sealed are in green and sealed ones are in blue. Vertical scale is 1/5000 and horizontal scale is 1/1000.

6. INTERPRETATION OF THERMAL PROFILE AND CONVECTIVE CELLS

Fracture zones in the Muschelkalk and in the Buntsandstein have been highlighted in GPK-2, GPK-3 and GPK-4 at Soultz. Above these formations, i.e. between the Tertiary formations and the lower part of the Upper Trias (Keuper), there is no obvious evidence of permeable or sealed fractures from mud logging and well logging data excepted in GPK-1, where two permeable fracture zones were located in Keuper formation. Below the Triassic formations, in the granitic basement, the permeable or sealed fracture zones are widely documented. This fracture network controls the convection, especially from 1400 to 3500 m deep in the granite (Figure 2). Between top of Keuper and bottom of *Vosgian* Sandstones, permeability structure is mainly complex fracture zone located in Middle and Upper Muschelkalk and in the Lower *Vosgian* sandstones. According to caliper data and instantaneous well logging, we interpreted those structures as large scale fault zones. As they are systematically visible in all wells, they show a spatial continuity as well as a hydraulic continuity due to the mud losses occurrences. As they are located in URG, those fault zones present a vertical apparent offset suggesting a large extension. Thus, a large scale fault cross cutting the Buntsandstein is probably connected to other large scale fault cross cutting the Muschelkalk.

Based on this structural analysis of fault system at the sediments/basement interface in the URG, we propose a conceptual model of the convective cell structure (Figure 11). In equilibrium temperature conditions, the conduction regime is dominant in the sedimentary formations from Tertiary, Jurassic and top of Trias (0-800 m deep). Within the deepest Mesozoic sedimentary formations (Muschelkalk, Buntsandstein) and in the granitic basement, heat transport process is dominated by the convection. The depth section 880-1000 m, i.e. the top of the Muschelkalk and the transition to the Buntsandstein, presents permeable fracture zones

and corresponds to a thermal regime governed by conduction. This indication suggests that this zone is the top of the convective cells and fluids cannot move upward within the fractures located above the Muschelkalk formations. The horizontal bounding layer at the top of the convective cell could fit with Keuper formation (Upper Trias).

The lower part of the convective cells initiates at about 3.5 km deep in the fractured and altered granite. The hydrothermal fluids percolate within the sub-vertical fault system and ascend until the Mesozoic formations such as Muschelkalk and Buntsandstein at circa 900 m deep. The fluids are stopped by a lithological and thermal screen called cap rock and formed by post-Muschelkalk sedimentary formations. Those rather impermeable top bounding layers with very large rock heat capacity simulate low permeability layers such as claystones that allow heat, but not mass transfer out of the reservoir.

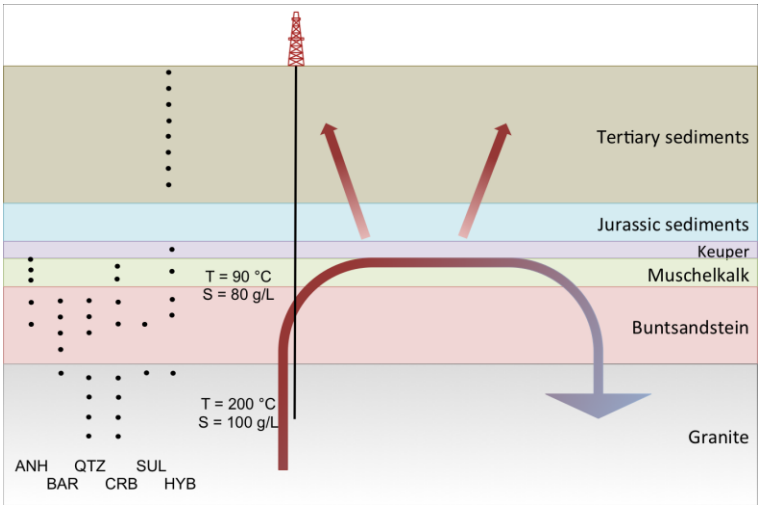

Figure 11: Schematic section through the convective cells in the sedimentary and granitic reservoirs. Geothermal fluid circulations are controlled by fracture network in the Muschelkalk, Buntsandstein formations and crystalline basement. During circulation, secondary mineral deposits occur in the fractures (ANH= Anhydrite, QTZ = Quartz, CRB = Carbonates, SUL = Sulfides, BAR = Barite). The uppermost part of the sedimentary cover remains highly conductive and insulates the convective system below. Hydrocarbons (HYB) are mostly located in the Triassic sediments. Values of temperatures and salinity of brine are from Soultz geothermal wells.

The cap rock development could be re-enforced by geochemical fluid-rock interaction process generating minerals deposition and sealing. During brine circulation, heavy minerals are deposited in fracture network (Figure 11). The nature of deposits varies in geological layers. In granite and Buntsandstein, secondary quartz and carbonates as calcite were observed in fractures on core samples of EPS-1 and GPK-1. Some sulfides as galena were present in lower amounts. Barite is characteristic of hydrothermal filling of fracture zones in Buntsandstein. Anhydrite has been detected in fracture zones affecting sedimentary layers, mostly in Muschelkalk and also Buntsandstein. In fractures in Muschelkalk, anhydrite is associated to calcite (Vernoux et al., 1995).

The cap rock is composed by the uppermost sedimentary section till 786 m deep, corresponds to Tertiary, Jurassic and late Triassic layers. Tertiary is made of Oligocene and Eocene sediments. The theory of the cap rock insulating the more brittle underlying formations (limestones from Muschelkalk, sandstones from Buntsandstein, Paleozoic granite), underlines the contrast of rheology of the two units. In the soft sediments of the cap rock, the development of the brittle faults is difficult. In the brittle formations below 1 km deep, natural fractures are developed through geological times allowing hydrothermal fluids circulation (permeability) and also secondary minerals deposits (sealing). The thermal regime observed may be linked to the petrophysical and rheological properties of the rocks. The conduction process is dominant in soft rocks with a low competence like marls, oil formations or clays from Tertiary and Jurassic or dolomites and anhydrites from Late Trias, whereas convection is dominant in hard formations.

7. CONCLUSION

Combined mud logging and well logging data analysis in the sedimentary cover of several geothermal wells in the Upper Rhine Graben (URG) in the Soultz site reveals the occurrences of fracture zones in Triassic sedimentary formations. Those fracture zones are made of individual or complex structure and the latest characterized probably by faulted zones cross-cutting the deepest sediments of the Tertiary basin. Based on mud losses occurrences, it has been shown that fracture permeability is associated mainly to complex fracture zones located in the Middle Muschelkalk limestone and Middle Buntsandstein sandstones. At borehole-scale, many fracture zones are sealed due to the occurrence of secondary mineral precipitations.

The natural permeability in the sub-vertical fracture zone evidenced the geothermal fluid pathways. A schematic conceptual model of the top of convective cell has been proposed which delineated that natural fluids move upward from the top crystalline to those Triassic sediments. Complex permeable fracture zones are probably connected to large scale fault and small-scale fracture network at the sediment/basement interface and control the top of thermal convection.

ACKNOWLEDGEMENTS

A part of this work was done in the framework of the Labex G-Eau-Thermie Profonde which is co-funded by the French government under the program “Investissements d'Avenir”. The authors acknowledge the GEIE EMC and the LIAG for providing Soultz boreholes data and Dr Nicolas Cuenot and Dr Thomas Koelbel for support.

REFERENCES

Baechler D., Kohl T., and Rybach L.: Impact of graben-parallel faults on hydrothermal convection–Rhine Graben case study, *Physics and Chemistry of the Earth*, **28**, (2003), 341–441.

Baillieux P., Schill E, Edel J-B, and Mauri G.: Localization of temperature anomalies in the Upper Rhine Graben: insights from geophysics and neotectonic activity, *International Geology Review*, (DOI: 10.1080/00206814.2013.794914), (2013).

Baumgärtner J. and Lerch C.: Geothermal 2.0: The Insheim Geothermal Power Plant. the second generation of geothermal power plants in the Upper Rhine Graben, *Proceedings*, Third European Geothermal Review, Third European Geothermal Review, (June 2013).

Baumgärtner J., Moore P.L., and Gérard A.: Drilling of hot and fractured granite at Soultz-sous-Forêts, *Proceedings*, World Geothermal Congress 1995, Florence, Italy, (1995).

Baumgärtner J., Gérard A., and Baria R.: Soultz-sous-Forêts: main technical aspects of deepening the well GPK-2, *Proceedings*, World Geothermal Congress 2000, Kyushu - Tohoku, Japan, (May-June 2000).

Baumgärtner J., Teza D., Hettkamp T., Homeier G., Baria R., and Michelet S.: Electricity production from hot rocks, *Proceedings*, World Geothermal Congress 2005, Antalya, Turkey, (April 2005).

Benderitter Y. and Elsass Ph.: Structural control of deep fluid circulation at the Soultz HDR Site, France, *Geothermal Science and Technology*, (1995), 227–237.

Cautru J-P.: Coupe géologique passant par le forage GPK-1 calée sur la sismique réflexion, rapport interne, document BRGM, Technical report, Institut Mixte de Recherches Géothermiques, (1988).

Degouy M., Villeneuve B., and Weber R.: Logistical support and development of the Soultz Hot Dry Rock site: seismic observation wells and well EPS-1, final drilling report, Technical Report RR-41179-FR, BRGM, CFG 009, Comission of European Communities, (February 1992).

Dezayes C., Genter A., and Valley B.: Structure of the low permeable naturally fractured geothermal reservoir at Soultz, *Comptes Rendus Geoscience*, **342**, (2010), 517–530.

Evans K., Genter A., and Sausse J.: Permeability creation and damage due to massive fluid injections into granite at 3.5km at Soultz, *Journal of Geophysical Research*, **110** (B04203, doi: 10.1029/2004JB003168), (2005).

Genter A.: Géothermie roches chaudes sèches: le granite de Soultz-sous-Forêts (Bas-Rhin, France). Fracturation naturelle, altérations hydrothermales et interaction eau-roche, Document du BRGM 185, PhD thesis, Université d'Orléans, France, (1989).

Genter A. and Traineau H. Borehole EPS-1, Alsace, France: preliminary geological results from granite core analyses for Hot Dry Rock research. Scientific Drill, (3): 205–214, 1992.

Genter A. and Traineau H.: Analysis of macroscopic fractures in granite in the HDR geothermal well EPS-1, Soultz-sous-Forêts, France, *Journal of Volcanology and Geothermal Research*, **72**, (1996), 121–141.

Genter A., Castaing C., Dezayes C., Tenzer H., Traineau H., and Villemin T.: Comparative analysis of direct (core) and indirect (borehole imaging tools) collection of fracture data in the Hot Dry Rock Soultz reservoir (France), *Journal of Geophysical Research*, **102(B7)**, (1997), 15419–15431.

Genter A., Traineau H., Ledésert B., Bourgine B., and Gentier S.: Over 10 years of geological investigations within the HDR Soultz project, France, *Proceedings*, World Geothermal Congress 2000, Kyushu - Tohoku, Japan, (May-June 2000).

Genter A., Evans K., Cuenot N., Fritsch D., and Sanjuan B.: Contribution of the exploration of deep crystalline fractured reservoir of Soultz to the knowledge of Enhanced Geothermal System (EGS), *Comptes Rendus Geoscience*, **342**, (2010), 502–516.

Genter A., Cuenot N., Melchert B., Moeckes W., Ravier G., Sanjuan B., Sanjuan R., Scheiber J., Schill E., and Schmittbuhl J.: Main achievements from the multi-well EGS Soultz project during geothermal exploitation from 2010 and 2012, *Proceedings*, European Geothermal Congress 2013, Pisa, Italy, (June 2013).

Gérard A., Genter A., Kohl T., Lutz Ph., Rose P., and Fritz R.: The deep EGS (Enhanced Geothermal System) project at Soultz-sous-Forêts (Alsace, France), *Geothermics*, **35**, (2006), 473–483.

Guillou-Frottier L., Carré C., Bourgine B., Bouchot V., and Genter A.: Structure of hydrothermal convection in the Upper Rhine Graben as infered from corrected temperature data and basin-scale numerical models, *Journal of Volcanology and Geothermal Research*, **256**, (2013), 29–49.

Haffen S., Géraud Y., Diraison M., and Dezayes C.: Determining fluid-flow zones in a geothermal sandstone reservoir from thermal conductivity and temperature logs, *Geothermics*, **48**, (2013), 32–41.

Herbrich B.: Le forage géothermique de Soultz-sous-Forêts (GPK-1), rapport de fin de sondage, Technical Report 29421, CFG 003, (1988).

Hettkamp T., Baumgärtner J., Baria R., Gérard A., Gandy T., Michelet S., and Teza D.: Electricity production from hot rocks, *Proceedings*, Twenty-Ninth Workshop on Geothermal Reservoir Engineering, number SGP-TR-175, Stanford, California, (January 2004).

Hettkamp T., Baumgärtner J., Teza D., and Lerch C.: Experiences from 5 years operation in Landau, *Proceedings*, Third European Geothermal Review, Third European Geothermal Review, (June 2013).

Hooijkaas G.R., Genter A., and Dezayes C.: Deep-seated geology of the granite intrusions at the Soultz EGS site based on data from 5km-deep boreholes, *Geothermics*, **35**, (2006), 484–506.

Housse B-A.: Reconnaissance du potentiel géothermique du Buntsandstein à Strasbourg-Cronenbourg, *Géothermie Actualités*, **1**, (1984).

Kohl T., Baechler D., and Rybach L.: Steps towards a comprehensive thermo-hydraulic analysis of the HDR test site Soultz-sous-Forêts, *Proceedings*, World Geothermal Congress 2000, pages 2671–2676, Kyushu - Tohoku, Japan, (May-June 2000).

Kreuter C., Harthill N., Judt M., and Lehmann B.: Geothermal power generation in the Upper Rhine Valley, the project Offenbach/Pfalz, *Proceedings*, International Geothermal Conference 2003, Reykjavik, Island, (September 2003).

Le Carlier C., Royer J-J., and Flores L.E.: Convective heat transfer at the Soultz-sous-Forêts geothermal site: implications for oil potential, *First Break*, **12(11)**, (1994), 553–559.

Ledésert B., Joffre J., Amblès A., Sardini P., and Genter A.: Organic matter in the Soultz HDR granitic thermal exchanger (France): natural tracer of fluid circulations between the basement and its sedimentary cover, *Journal of Volcanology and Geothermal Research*, **70**, (1996), 235–253.

Ménillet F.: Notice de la carte géologique 1/50000 de Haguenau, In Carte géologique de la France, Service géologique national. BRGM, (1976).

Person M. and Garven G.: Hydrologic constraints on petroleum generation within continental rift basins: theory and application to the rhine graben, *AAPG Bulletin*, **76(4)**, (1992), 468–488.

Pribnow D. and Clauser C.: Heat and fluid flow at the Soultz Hot Dry Rock system in the Rhine Graben, *Proceedings*, World Geothermal Congress 2000, Kyushu - Tohoku, Japan, (May-June 2000).

Pribnow D. and Schellschmidt R.: Thermal tracking of upper crustal fluid flow in the Rhine Graben, *Geophysical Research Letters*, **27**, (2000).

Rummel F., Haack U., and Gohn E.: Uranium, thorium and potassium content and derived heat production rate for Technical Report 6, 9 p., Ruhr Universität Bochum Yellow Reports, (1988).

Schellschmidt R. and Clauser C.: The thermal regime of the Upper Rhine Graben and the anomaly at Soultz, *Zeitschrift fu ̈r Angewandte Geologie*, **12**, (1996), 40–44.

Stober I. and Jodocy M.: Eigenschaften geothermischer Nutzhorizonte im abden-württembergischen und französischen Teil des Obberheingrabens, *Grundwasser - Zeitschrift der Fachsektion Hydrogeologie*, **14**, (2009), 127–137.

Stober I. and Jodocy M.: Hydrochemical characteristic of deep seated waters in the Upper Rhine Graben, Basic information for geothermal energy, *Zeitschrift für Geologische Wissenschaften, Berlin*, **39**, (2011), 39–57.

Stussi J-M., Cheilletz A., Royer J-J., Chèvremont Ph., and Gilbert F.: The hidden monzogranite of Soultz-sous-Forêts (Rhine Graben, France), mineralogy, petrology and genesis, *Géologie de la France*, **1**, (2002), 45–64.

Vernoux J-F., Genter A., Razin Ph., and Vinchon C.: Geological and petrophysical parameters of a deep fractured sandstone formation as applied to geothermal exploitation: EPS-1 borehole, Soultz-sous-Forêts, France, Technical Report R 38622, BRGM, (1995).

Villadangos G.: ECOGI, EGS Upper Rhine Geothermal project for the industry, first well and result, *Proceedings*, Third European Geothermal Review. Third European Geothermal Review, (June 2013).

Vuataz F-D., Brach M., Criaud A., and Fouillac Ch.: Geochemical monitoring of drilling fluids: a powerful tool to forecast and detect formation waters. SPE, Formation Evaluation, pages 177–184, (1990).